Role of surrounding soils and pore water in calcium carbonate precipitation in railway tunnel drainage system

Zilong Wu, Yu-Jun Cui, Antoine Guimond Barrett, Miguel Mellado Moreno, Yongfeng Deng

Role of surrounding soils and pore water in calcium carbonate precipitation in railway tunnel drainage system

Zilong Wu[1, 2], Yujun Cui[2*], Antoine Guimond Barrett[3], Miguel Mellado Moreno[2], Yongfeng Deng[1]

1. *Southeast University, Institute of Geotechnical Engineering, School of Transportation, Nanjing, China*
2. *Ecole des Ponts ParisTech, Laboratoire Navier/CERMES, Marne-la-Vallée, France*
3. *SNCF-Réseau/Direction Ingénierie & Projets - Département des ouvrages d'art- Division Tunnels et Géotechnique*

Corresponding author

Prof. Yu-Jun Cui
Ecole des Ponts ParisTech
6-8 av. Blaise Pascal, Cité Descartes, Champs-sur-Marne
77455 Marne-la-Vallée cedex 2
France

Email: yu-jun.cui@enpc.fr
Phone: +33 1 64 15 35 50

Abstract

Calcium carbonate ($CaCO_3$) precipitation in tunnel drainage system poses serious problems to railway tracks. In this study, the calcification phenomenon identified in Meyssiez tunnel was analyzed through laboratory testing and site water monitoring. In particular, the surrounding soils were investigated in the laboratory. Site water table was regularly monitored in the field and site water was taken for laboratory analyses in terms of pH and electrical conductivity (EC). Examination of the test results showed that the calcification phenomenon was mainly induced by the calcium carbonate dissolution in the fine fractions (d < 0.08mm) of surrounding soils. Due to this dissolution, the void ratio of fine fractions (e_f) and the hydraulic conductivity (k) of soils both increased. Meanwhile, calcium carbonate dissolution increased the pH values and electrical conductivity (EC) of groundwater. However, any recharge of water table by rainfalls decreased both pH and EC. Further analysis showed that a calcium carbonate dissolution degree can be defined in terms of pH and/or electrical conductivity (EC) values. The lower the pH values or the higher the EC, the higher the calcium carbonate dissolution in surrounding soils.

Key words: tunnel drainage; calcium carbonate dissolution; fines fraction; pH values; electrical conductivity

1. Introduction

Railway has been one of the most important transportation means over the world. In France, more than 34000 km of rail lines have been constructed, including 6% of high-speed lines [1-2]. Nowadays, there are 1548 tunnels with a total length of 631 kilometers in the French railway network [3]. However, most of these tunnels have been affected by the calcification phenomenon [4-5]. This problem has been also involved in other countries, for instance, Switzerland [6], Austria [7], Korea [8] and China [9]. The calcium carbonate ($CaCO_3$) precipitation can cause clogging of tunnel drainage system, heavily increasing the cost of maintenance [2,7]. Therefore, better understanding the calcification phenomenon in tunnel drainage system is of paramount importance in railway maintenance.

Through investigations on some specific cases, Dietzel *et al.* (2008) [7] and Jung *et al.* (2013) [8] reported that this calcification phenomenon was induced by the degradation of concrete lining and shotcrete. Recently, Chen *et al.* (2019) [5] studied problematic tunnels with calcification in some countries (including France, Austria, Korea and China) and proposed that this phenomenon is mainly induced by the dissolution of calcium carbonate ($CaCO_3$) in the surrounding soils. Basically, when rain water infiltrates into underground through the fissures of surrounding soils, the H^+ and HCO_3^- in the water react with the calcium carbonate ($CaCO_3$) in the soils, leading to the generation of calcium bicarbonate (Ca^{2+} and HCO_3^-) [2,5,7,10], as shown in equation (1). As a result, the pH value and the electrical conductivity (EC) of groundwater increase. Meanwhile, progressive dissolution of calcium carbonate creates additional fissures, increasing the void ratio (e) and hydraulic conductivity (k) of surrounding soils.

$$CaCO_3 + H^+ + HCO_3^- \Leftrightarrow Ca^{2+} + 2HCO_3^- \quad (1)$$

Thereafter, the groundwater carrying Ca^{2+} and HCO_3^- flows through the soils, finally reaching the drainage gutters through the drain holes. As the external environment (air pressure in the tunnel and the temperature of drainage solutions) changes, reaction (1) would happen in the inversed direction, from right to left, causing calcium carbonate precipitation in tunnel drainage gutters [2,5,7].

It should be noted that the viewpoint of Chen *et al.* (2019) [5] was made based on a statistical analysis and needed to be verified by test results on both soil and water. This paper reports a detailed case study of Meyssiez Tunnel in France. After identification of the calcification in this tunnel, core samples of the surrounding soils were taken from the site for laboratory characterization. Field water table was also regularly monitored and site water was taken for laboratory analyses in terms of pH and electrical conductivity. The test results allowed the calcium carbonate ($CaCO_3$) dissolution in the surrounding soils to be identified as the main mechanism involved in the calcium carbonate precipitation in the tunnel drainage system.

2. Calcium carbonate precipitation in Meyssiez tunnel

Meyssiez tunnel is located near Meyssiez village, approximately 50 km south of Lyon, France. It was constructed in the period from 1990 to 1993 in the sedimentary limestone area and has a total length of 1878 m. The geology environment is shown in **Fig. 1**, indicating that the surrounding soils are mainly Mill-stone, Mill-sand and Mill-sandstone. Note that these soils all have a high content of limestone (up to 60%). The top layer involves a normal surface soil without limestone and its thickness changes with the locations: 12.7 m at the hillcrest and 5 m at the southern hill toe. **Fig. 2** shows the tunnel structure with concrete linings and shotcrete of 55 cm and 25 cm, respectively. Note that in order to decrease the water pressure applied on the structure, a number of drainage holes and

two lateral gutters were set up.

Meyssiez tunnel has been exploited for twenty-five years. Its drainage system has been seriously affected by calcium carbonate precipitation [4-5], as shown in **Fig. 3**. Dietzel *et al.* (2008) [7] and Jung *et al.* (2013) [8] concluded that this problem was induced by the degradation of shotcrete and concrete lining. Indeed, Laver *et al.* (2013) [11] conducted a series of tests on shotcrete samples extracted from London tunnel. Results revealed a greater permeability and an altered shotcrete composition in the older shotcrete samples (1902-1926s). However, this was not the case for the new shotcrete (1970s) [11]. Considering the construction date for Meyssiez tunnel (1990s-1993s), it is normal to ignore any degradation of the shotcrete of this tunnel. On the other side, the calcium carbonate precipitation in Meyssiez tunnel has been occurring since several years, without any noticeable change of the concrete lining state (leaking and cracking) based on the field investigations on this tunnel. Therefore, it can be concluded that the calcification phenomenon observed is not closely related to the shotcrete and concrete lining in Meyssiez tunnel. The responsible is most likely the surrounding soils.

3. Laboratory characterization of the surrounding soils and pore-water

3.1 Materials

The natural soil core with dimensions of 10 cm in diameter and 20 m in height was taken at 01/08/2017 by drilling at a location 50 m far from the south exit of Meyssiez tunnel. Thereafter, the soil core was sealed in plastic tubes with ends closed to avoid water loss by evaporation. After sampling, the borehole was kept as a piezometer for the monitoring of site water table and a source for groundwater sampling. The field monitoring of water table was undertaken every two weeks from 31/08/2017 to 07/06/2018, together with the groundwater sampling after each monitoring. Note that

when it was possible, the rainwater was also collected for the purpose of comparison. For both rainwater and groundwater, the pH and electrical conductivity (EC) were measured in the laboratory following American standard [12-13].

The basic parameters of soils at different depths are shown in **Fig. 4**. The natural water content (w_n) was determined by oven-drying. The liquid limit (*LL*) and plastic limit (*PL*) were measured using Casagrande method and rolling method, respectively [14]. The specific gravity (G_s) was determined following ASTM standard [15]. The sand content (w_s; $d \geq 0.08$ mm) and the fine fractions ($d < 0.08$ mm) were obtained by wet sieving [16]. The Calcium carbonate ($CaCO_3$) contents in surrounding soils (w_{caT}) and that in the fine fractions (w_{caf}) were measured following AFNOR standard [17].

Fig. 4 shows that the values of natural water content (w_n), liquid limit (*LL*), plastic limit (*PL*), natural density (ρ_n), specific gravity of soils (G_{sT}), specific gravity of fine fraction (G_{sf}) and sand content (w_s), equal to 7.8% to 24.6%, 34.9% to 72.8%, 16.9% to 28.8%, 1.55 Mg/m^3 to 2.09 Mg/m^3, 2.71 to 2.79, 2.73 to 2.80 and 8.16% to 75.6%, respectively. **Fig. 4** also reveals that in the soils at depths of 6.0 m, 7.3 m, 12.7 m and 15.4 m, the sand contents (w_s) exceed 60%, categorizing these soils into sandy soils. Therefore, their liquid limit (*LL*) and plastic limit (*PL*) could not be determined.

In addition, **Fig. 4** shows that w_{caT} and w_{caf} are equal to zero when the depth is less than 5 m, indicating that calcium carbonate does not exist in this zone. However, calcium carbonate is widely distributed beyond 5 m depth, in agreement with the geology environment shown in **Fig. 1**. **Fig. 4** also presents the change of R_{caT} and R_{caf} with the depth. The definitions of R_{caT} and R_{caf} are shown below:

$$R_{caT} = \frac{m_{caT}}{m_{sT}} * 100\% \quad (2)$$

$$R_{caf} = \frac{m_{caf}}{m_{sT}} * 100\% \quad (3)$$

where m_{caT} and m_{caf} refer to the mass of calcium carbonate ($CaCO_3$) in the total soils and fine fractions, respectively; m_{sT} is the total soil mass. It can be observed from **Fig. 4** that R_{caT} is close to R_{caf}, suggesting that the calcium carbonate is mostly distributed in the fine fractions of surrounding soils.

According to *LL* and *PI*, the classification of soils is obtained and shown in **Fig. 5**. Meanwhile, through the visual observation of soil color, the soil layer distribution at this site (from 0-20 m) was determined and is shown in **Fig. 4**. It reveals that the normal surface soils (0-5 m) are mainly gravel, high-plasticity clay (M-CH) and low-plasticity clay (M-CL). For the soil layers below 5 m, they mainly consisted of Millsand, Millclays.

3.2 Void ratio and hydraulic conductivity

To measure the void ratio (e) and hydraulic conductivity (k) of natural soils at different depths, a steel sampler with dimensions of 18 mm in height and 70 mm in diameter was used for the preparation of specimens. Thereafter, these soil specimens in the steel sampler were carefully introduced into an oedometer cell. Note that the inner wall of the cell was lubricated in advance with grease to avoid water infiltration between soil samples and the cell. Prior to hydraulic conductivity measurement, the in-situ effective stress σ_v' calculated by equation (4) was applied on the soil specimens with recording of the vertical displacement, as shown in **Fig. 6**.

$$\sigma_v' = \sum_{i=1}^{n} \gamma_i' h_i \quad (4)$$

In equation (4), σ_v' is the effective in-situ stress, (kPa); n stands for the number of soil layers; h

refers to the depth of soil (m). When h is less than 7.50 m (corresponding to the groundwater level at sampling time of 01/08/2017), the γ_i' was taken equal to the bulk unit weight γ_i (kN/m^3). If h exceeds 7.50 m, the γ_i' is the buoyant unit weight (kN/m^3).

Note that in the loading process, the equilibrium state was regarded as reached when the vertical displacement rate was lower than 0.01 mm every 8 h [18-20]. After loading, a constant water pressure of 20 kPa was applied from the lower base of cell for the sample saturation. The vertical displacement was monitored in this process (shown in **Fig. 6**). When the deformation stabilized, the hydraulic conductivity (k) was measured using the constant water head method [21]. Based on the experimental data, the final void ratio (e) and hydraulic conductivity (k) were calculated by:

$$e_0 = \frac{G_{sT}(1+w_n)\rho_w}{\rho_n} - 1 \tag{5}$$

$$e = e_0 - \frac{\Delta h}{H_0}(1+e_0) \tag{6}$$

$$k = \frac{QH_f}{AH_w t} \tag{7}$$

where e_0 and e refer to the initial and final void ratios of soil specimens; G_{sT} is the specific gravity of soils; w_n stands for natural water content, (%); ρ_w and ρ_n are the unit masses of water and natural soil, respectively, (Mg/m^3). Δh is the total displacement of samples in the loading and saturation process, (m); H_0 and H_f are the initial and final heights of samples respectively, (m). Q is water volume injected, (m^3); A refers to the of samples' section, (m^2); H_w stands for the water head applied, (m); t is the elapsed time, (s).

3.3 Void ratio

Normally, with the calcium carbonate dissolution, the total void ratio e of soils increases. To investigate this point, the relationship between total void ratio (e) and calcium carbonate content

(w_{caT}) in total soils is established and shown in **Fig. 7 (*a*)**. As the soils located above 5 m do not contain any calcium carbonate (shown in **Fig. 4**), the data of these soils is excluded in further analysis.

Fig. 7 (*a*) reveals that the total void ratio e increases gradually with the decrease of w_{caT} due to the calcium carbonate dissolution. It is worth noting that due to the data scatter the fitting line shown in **Fig. 7 (*a*)** has a low regression coefficient R^2 (equal to 0.35). Considering that the calcium carbonate mostly exist in the fine fractions (d < 0.08mm; shown in **Fig. 4**), the calcium carbonate dissolution must mainly affect the change of void ratio of fine fractions (e_f). To determine e_f, a four-phase model [22-28] shown in **Fig. 8** is adopted, where the void ratio of fine fractions (e_f) is defined as the ratio of void volume (V_v) to the fine fraction volume (V_f), calculated by the following equations:

$$\rho_{df} = \frac{(w_f/100)\rho G_{ss}\rho_w}{G_{ss}\rho_w(1+w/100)-\rho(1-w_f/100)} \tag{8}$$

$$e_f = \frac{G_{sf}\rho_w}{\rho_{df}} - 1 \tag{9}$$

where ρ_{df} is the dry unit mass of fine fractions, (Mg/m^3); w_f stands for the fine fraction (in dry mass, %); ρ is the unit mass of soil samples after saturation, (Mg/m^3); ρ_w denotes the unit mass of water, (Mg/m^3); w is the water content of samples after saturation, (%); G_{sf} is the specific gravity of fine fractions; G_{ss} refers to the specific gravity of sand, which is calculated by the weighted average method. Note that in case of pure fine soils, the fine fraction (w_f) is equal to 100; the ρ_{df} and e_f shown in Eq. (1) and Eq. (2) become total dry densityρ_d and total void ratio e of pure fine soils, respectively. If the fine fraction (w_f) is equal to 0, the soil is pure sand and the ρ_{df} and e_f are equal to 0.

Fig. 7 (*b*) shows the change of e_f with the calcium carbonate content in the fine fraction w_{caf}. It is observed that there is a satisfactory correlation between e_f and w_{caf}, and the regression coefficient (R^2) is as high as 0.81. **Fig. 7 (*b*)** also reveals that e_f increases progressively with the decrease of w_{caf},

indicating the effect of calcium carbonate dissolution in the fine fractions.

3.4 Hydraulic conductivity

Fig. 9 (*a*) shows the change of hydraulic conductivity k with calcium carbonate content w_{caT} in the semi-logarithm plane. It is observed that the hydraulic conductivity k increases with the decrease of w_{caT}. This is consistent with the increase of total void ratio e by the calcium carbonate dissolution. It is worth noting that due to the data scatter the regression coefficient R^2 of fitting line is as low as 0.54.

Indeed, the calcium carbonate ($CaCO_3$) mostly exists in the fine fractions of surrounding soils, and the calcium carbonate dissolution mainly increases the void ratio of fine fractions (e_f) (shown in **Fig. 7 *b***), which finally leads to the increase of hydraulic conductivity k. This can be obviously proven from **Fig. 9 (*b*)**. Note that the fitting line shown in **Fig. 9 (*b*)** has a regression coefficient R^2 as high as 0.88, suggesting that calcium carbonate dissolution mainly occurred in the fine fractions.

3.5 Water pH value

Fig. 10 shows the changes of pH values ($pH=-\log H^+$) and water level with the sampling date. It is observed that the measured pH values of groundwater range from 6.6 to 7.6, which is higher than that of rainwater (5.6), suggesting that calcium carbonate dissolution occurred in soil pore water, because in this process the H^+ in water is consumed and the pH value increases accordingly (see Eq. 1). This is confirmed by the comparison between the change of pH and the change of water table (**Fig. 10**). Indeed, in general the pH values of groundwater decrease over the sampling time, but this change is not totally compatible with the change of groundwater level: with rainfalls that recharge the groundwater, the concentration of H^+ in the groundwater increases because of the higher H^+ concentration ($1\times10^{-5.6}$) and lower pH value (5.6) of the rainwater, leading to the decrease of pH

values. However, punctually, increase of pH occurred with the increase of groundwater level. This suggests that the pH values are not only affected by the increase of H^+ concentration through the recharge of groundwater, but also by the calcium carbonate dissolution.

To further investigate the change of pH values, a characteristic pH values (pH_c) is defined that excludes the calcium carbonate dissolution, using the model shown in **Fig. 11**. It is worth noting that in the calculation process, the H^+ concentration ($pH=-\log H^+$) and water volume ($V_w = \pi \times r^2 \times (20-7.53)$) at point A (shown in **Fig. 10**) are considered. When the groundwater level increases from D to E, the added H^+ and rainwater volume can be determined, and then the characteristic pH value (pH_c) at point B can be calculated by superposition. When the groundwater level decreases from E to F or remains unchanged, the pH_c values at point C is kept the same as that at point B, although the water volume at the borehole decreases. Adopting the above method, the pH_c values were calculated for the whole monitoring period. Note that the calcium carbonate content in the soils located above 5m is zero (**Fig. 4**). Meanwhile, the hydraulic conductivity of soils between 5 m to 7.2 m (the average groundwater level) is as high as 10^{-3} m/s (**Fig. 9**). Therefore, the calcium carbonate dissolution between rainwater and surrounding soils in the water infiltration process is neglected.

Fig. 10 shows the comparison between the measured and the characteristic pH values. It is observed that the pH_c values are lower than the measured ones (pH_m), suggesting that a higher H^+ concentration is obtained by excluding the calcium carbonate dissolution process, indirectly confirming the occurring of calcium carbonate dissolution. **Fig. 10** also reveals that the difference between these two values is quite small at high pH values (corresponding to high pHc value/low H+ concentration) and quite large at low pH values (corresponding to low pHc value/high H+

concentration). This difference corresponds to the degree of calcium carbonate dissolution, defined as follows:

$$D_{Dp} = \frac{pH_m - pH_c}{pH_c} \quad (10)$$

Fig. 12 shows the change of calcium carbonate dissolution degree (D_{Dp}) with pH values. It is observed that the dissolution degree D_{Dp} is strongly correlated to pH. The higher the pH in groundwater, the lower the D_{Dp} in surrounding soils.

3.6 Water electrical conductivity

Fig. 13 shows the change of electrical conductivity (EC) and groundwater level over the sampling time. It is observed that the EC of groundwater ranges from 4.6 us/m to 6.6 us/m, higher than that of rainwater (0.45 us/m). This difference is also caused by the calcium carbonate dissolutions. Due to this reaction, the calcium bicarbonate (Ca^{2+} and HCO_3^-) are generated and entered in groundwater, resulting in the increase of EC. **Fig. 13** also reveals that the EC of groundwater has an increase trend over the sampling time. But the change pattern of EC is different from that of groundwater level, suggesting that EC was affected by both the change of groundwater level and the calcium carbonate dissolution. With rainfalls, groundwater was recharged; the concentrations of Ca^{2+} and HCO_3^- were expected to decrease by dilution, leading to a decrease of EC. On the other hand, through the calcium carbonate dissolution process, the concentrations of Ca^{2+} and HCO_3^- in water were expected to increase, leading to the increase of EC. The general increase observed from **Fig. 13** shows that in the monitoring period, the dissolution process prevailed over the dilution process.

Adopting the similar model shown in **Fig. 11**, the characteristic electrical conductivity (EC_c) can be also calculated that excludes the calcium carbonate dissolution. The results are shown in **Fig. 13**. It is observed that most of the EC_c values are lower than the measured ones (EC_m), except some

points in the beginning of the monitoring period, probably due to the hydrogeological environment. This confirms that calcium carbonate dissolution was the prevailing mechanism over the monitoring period. In general, the difference between the calculated and the measured EC is larger at higher EC values (corresponding to lower EC_c/more rainfall/high H^+ concentration). This difference can be also defined as the dissolution degree of calcium carbonate (D_{DE}), as follows:

$$D_{DE} = \frac{EC_m - EC_c}{EC_c} \tag{11}$$

Fig. 14 shows the change of calcium carbonate dissolution degree (D_{DE}) with the electrical conductivity (EC). A general increase trend of D_{DE} with the increase of EC can be observed. **Fig. 15** shows the comparison between D_{Dp} and D_{DE}. Interestingly, a very close relationship is observed between the two parameters, suggesting that both EC and pH can be used as indicator of the calcium carbonate dissolution occurred in surrounding soils/pore water.

4. Conclusions

A case study of Meyssiez Tunnel was conducted. After identification of the calcium carbonate precipitation in this tunnel, surrounding soil samples were taken from the site for laboratory characterization. The groundwater table was also monitored in the field and both pore-water and rain water were taken for laboratory analyses in terms of pH and electrical conductivity. Results obtained allow the following conclusions to be drawn.

(1) The calcium carbonate precipitation in tunnel drainage system was mainly induced by the dissolution of calcium carbonate in the fine fractions (d < 0.08 mm) of surrounding soils. Due to this dissolution, both the void ratio of fine fractions (e_f) and the hydraulic conductivity (k) of soils increased.

(2) Calcium carbonate dissolution increased the pH values of groundwater. However, any

recharge of water table decreased pH values through increasing the H^+ concentration in water. A model was proposed for calculating the characteristic pH value (pH_c), excluding the effect of calcium carbonate dissolution. Results show a significant difference between the measured and characteristic pH values, indirectly confirming the occurring of calcium carbonate dissolution. A calcium carbonate dissolution degree was defined, showing that the higher the pH value (corresponding to a high pHc value/low H+ concentration), the lower the calcium carbonate dissolution in the surrounding soils.

(3) Calcium carbonate dissolution increases the electrical conductivity (EC) of groundwater. However, the recharge of groundwater table decreases EC through the dilution of ions in water. It is found that the difference between measured EC value and the characteristic one (EC_c) determined using a proposed model is significant, suggesting the occurring of calcium carbonate dissolution. The calcium carbonate dissolution degree defined based on the measured and calculated EC values showed that the higher the EC value (corresponding to a lower ECc/more rainfall/high H+ concentration), the higher the calcium carbonate dissolution in the soils. Interestingly, this calcium carbonate dissolution degree is found to be well correlated with the one defined with pH values, indicating that both EC and pH can be used as indicator of the calcium carbonate dissolution occurred in surrounding soils/pore water.

Note that the calcium carbonate dissolution degree is an important index in practice because it can be used to approximately estimate the dissolution amount every year. Subsequently, the amount of CaCO3 precipitated in the tunnel gutters can be estimated.

Acknowledgments

The supports from Chinese Scholar Council (CSC) and the French Railway Company (SNCF) are

greatly appreciated. The first author is also grateful to Jiang Bo (Lecturer, QingDao University of Technology), Zeng Zhixiong (PhD candidate, ENPC), Qi Shuai (PhD candidate, Zhejiang University) and Wang Hao (PhD candidate, ENPC) for their useful suggestions.

Appendix A. Supplementary data

Data will be made available on request

References

[1] Cui YJ, Lamas-Lopez F, Trinh VN, Calon N, Costa D'Aguiar S, Dupla JC, Tang AM, Canou J, Robinet A. Investigation of interlayer soil behaviour by field monitoring. Transp Geotech 2014;1(3):91-105.

[2] Jia N, Tassin B, Calon N, Deneele D, Koscielny M, Prevot F. Scaling in railway infrastructural drainage devices: site study. Innov Infrastruct Solut 2016;1(42):1-11.

[3] Chille F, Sage-Vallier B, Guimond-Barrett A. Presentation for IN2 TRACK-WP4-Research into enhanced tracks, switches and structures (Internal SNCF document). 2016.

[4] Lassalle S. Calcification of drainage water in the tunnels of the Mediterranean LGV by using stabling pellets (internal SNCF document). 2012.

[5] Chen YF, Cui YJ, Guimond-Barrett A, Chille F, Lassalle S. Investigation of calcite precipitation in the drainage system of railway tunnels. Tunn Undergr Space Technol 2019;84:45-55.

[6] Gamisch T, Girmscheid G. Future Trends in Construction and Maintenance Management of Drainage Systems in Traffic Tunnels. 12th Australian Tunnelling Conference, Brisbane, Australia. 2005.

[7] Dietzel M, Rinder T, Leis A, Reichl P, Sellner P, Draschitz C, Plank G, Klammer D, Schöfer H. Koralm tunnel as a case study for sinter formation in drainage systems-precipitation

mechanisms and retaliatory action. Geomechanics Tunn 2008;4:271-278.

[8] Jung HS, Han YS, Chung SR, Chun BS, Lee YJ. Evaluation of advanced drainage treatment for old tunnel drainage system in Korea. Tunn Undergr Space Technol 2013;38:476-486.

[9] Zhai M. Study on the regularity of crystallization and blocking of tunnel drainage system in limestone area. Master's thesis. Chongqing Jiaotong University. 2016.

[10] Nia MG, Rahimi H, Sohrabi T, Naseri A, Tofighi H. Potential risk of calcium carbonate precipitation in agricultural drain envelopes in arid and semi-arid areas. Age Water Manage 2010;97:1602-1608.

[11] Laver RG, Soga K, Wright P, Jefferis S. Permeability of aged grout around tunnels in London. Geotechnique 2013;63(8):651-660.

[12] American Society for Testing and Materials (ASTM), 1999. Standard Test Methods for Electrical Conductivity and Resistivity of Water. ASTM. Soil and Rock, West Conshohocken, PA. D1125.

[13] American Society for Testing and Materials (ASTM), 2001. Standard Test Method for pH of soils. ASTM. Soil and Rock, West Conshohocken, PA. D1125.

[14] American Society for Testing and Materials (ASTM), 2010. Standard test methods for liquid limit, plastic limit, and plasticity index of soils. ASTM. Soil and Rock, West Conshohocken, PA. D4318.

[15] American Society for Testing and Materials (ASTM), 2014. Standard test methods for specific gravity of soil solids by water pycnometer. ASTM. Soil and Rock, West Conshohocken, PA. D4318.

[16] French Standardization Association (AFNOR), 2005. Geotechnical investigating and testing,

Laboratory testing of soils. Part 4: Determination of particle size distribution. AFNOR. P94.

[17] French Standardization Association (AFNOR), 1996. Soil : investigation and testing-Determination of the carbonate content-Calcimeter method. AFNOR. P94.

[18] French Standardization Association (AFNOR), 2005. Geotechnical investigating and testing, Laboratory testing of soils. Part 5: Incremental loading oedometer test. AFNOR. P94.

[19] Deng YF, Tang AM, Cui YJ, Nguyen XP, Li XL, Wouters L. Laboratory Hydro-Mechanical Characterisation of Boom Clay at Essen and Mol. Phys Chem Earth 2011;36:1878-1890. 2011.

[20] Deng YF, Cui YJ, Tang AM, Li XL, Sillen X. An experimental study on the secondary deformation of Boom clay. Appl Clay Sci 2012;59-60:19-25.

[21] French Standardization Association (AFNOR), 2005. Geotechnical investigating and testing, Laboratory testing of soils. Part 11: Determination of permeability by constant and falling head. AFNOR. P94.

[22] Dixon DA, Gray MN, Thomas AW. A study of the compaction properties of potential clay-sand buffer mixtures for use in nuclear fuel waste disposal. Eng Geol 1985;21(3):247-255.

[23] Lee JO, Cho WJ, Chun KS. Swelling pressures of a potential buffer material for high-level waste repository. J Kor Nucl Soc 1999;31(2):139-150.

[24] Wang Q, Tang AM, Cui YJ, Delage P, Gatmiri B. Experimental study on the swelling behavior of bentonite/claystone mixture. Eng Geol 2012;124:59-66.

[25] Wang Q, Tang AM, Cui YJ, Delage P, Barnichon JD, Ye WM. The effect of technological voids on the hydro-mechanical behavior of compacted bentonite-sand mixtures. Soils Found 2013;53(2):232-245.

[26] Chu CF, Wu ZL, Deng YF, Chen YG, Wang Q. Intrinsic compression behavior of remolded

sand-clay mixture. Can. Geotech J 2017;54:926-932.

[27] Deng YF, Wu ZL, Cui YJ, Liu SY, Wang Q. Sand fraction effect on hydro-mechanical behavior of sand-clay mixture. Appl Clay Sci 2017;135:355-361.

[28] Wu ZL, Deng YF, Cui YJ, Chen YG, Wang Q, Feng, Q. Investigations on secondary compression behaviours of artificial soft sand-clay mixtures. Soils Found 2019;59(2):326-336.

List of Figures

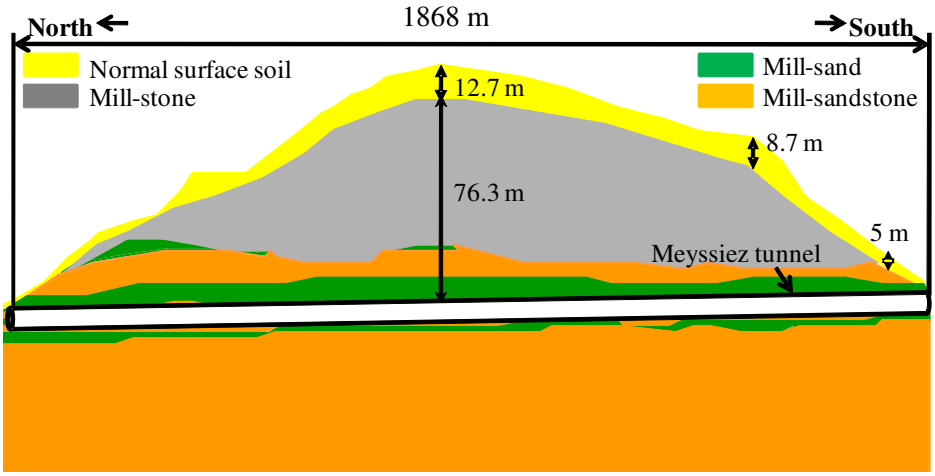

Fig. 1 Geology around the Meyssiez tunnel

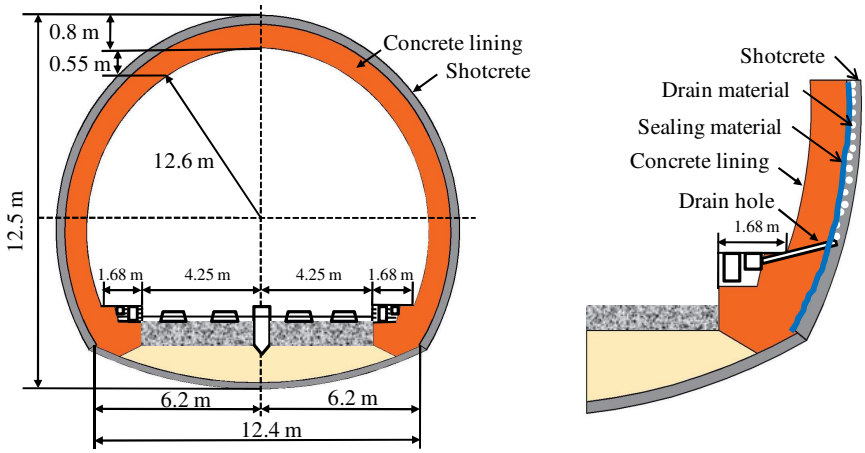

Fig. 2 Tunnel structure and drainage system

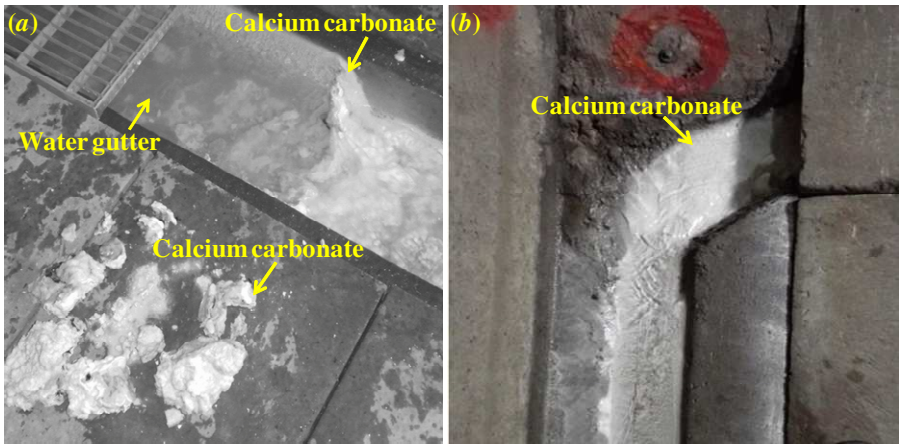

Fig. 3 Calcium carbonate precipitation in Meyssiez tunnel

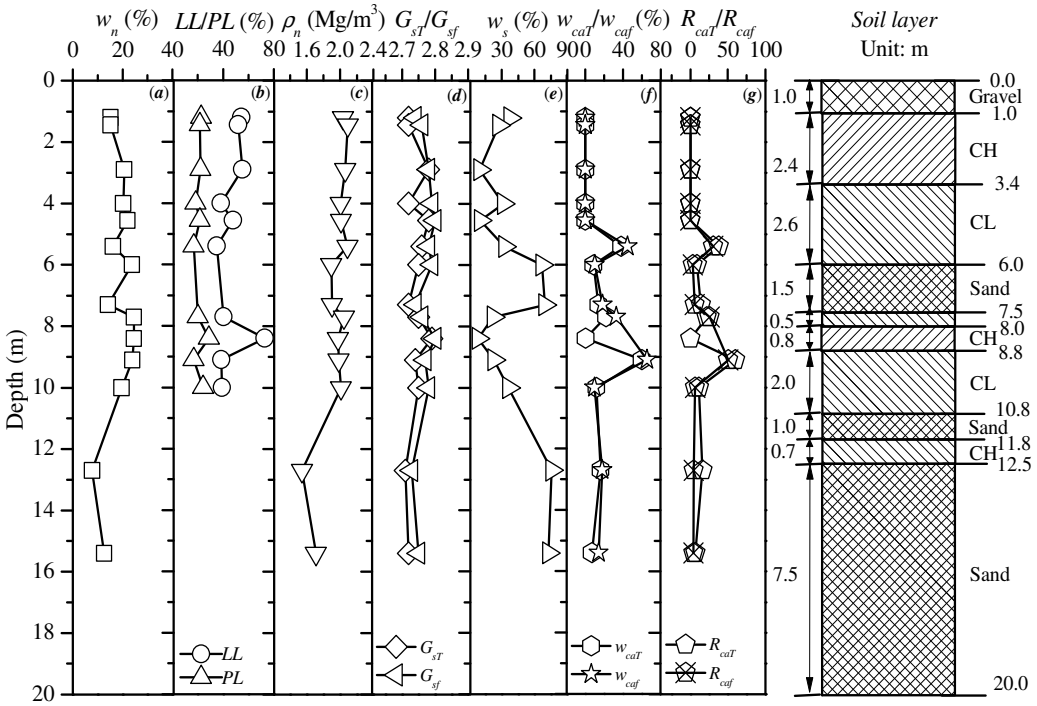

Fig. 4 Soil layers description and the profiles of basic parameters

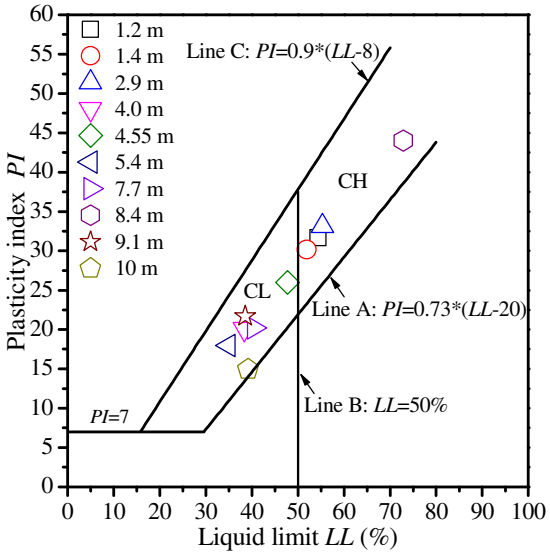

Fig. 5 Plasticity Chart

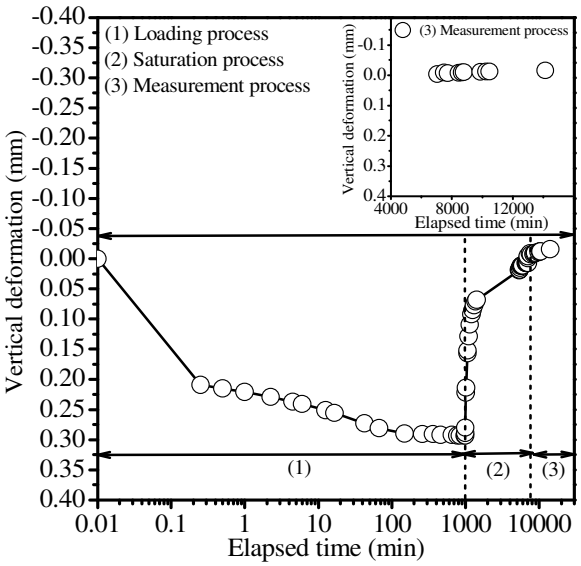

Fig. 6 Change of vertical displacement with elapsed time

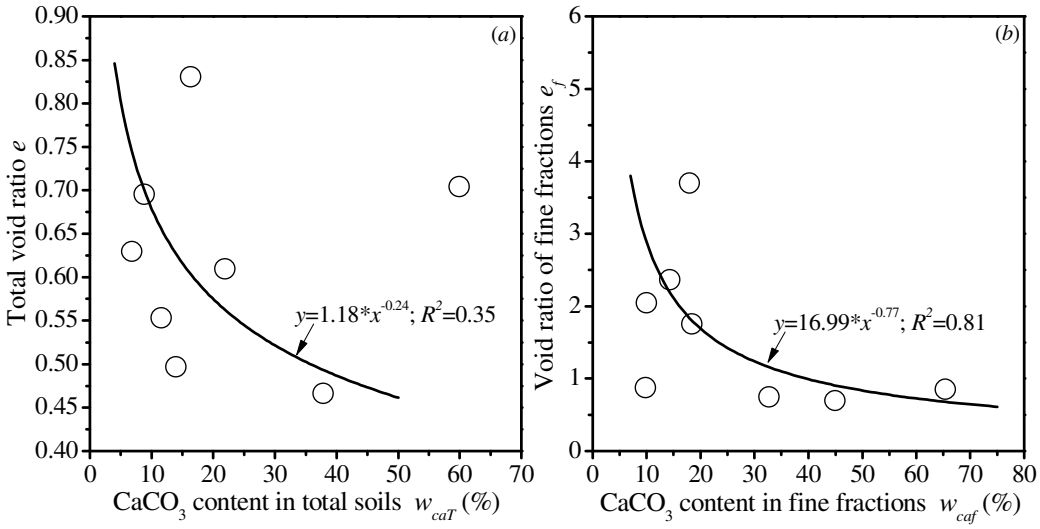

Fig. 7 Void ratio *vs* calcium carbonate content: (*a*) *e vs* w_{caT}; (*b*) e_f *vs* w_{caf}

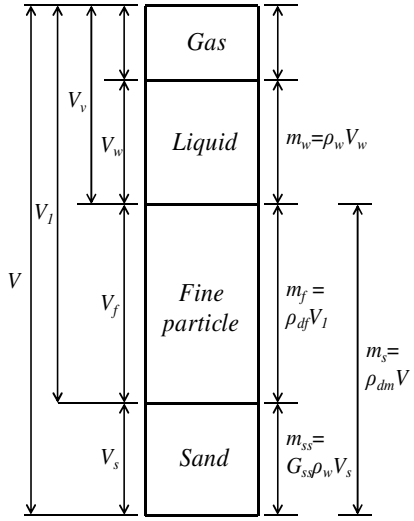

Fig. 8 Four-phase analysis model

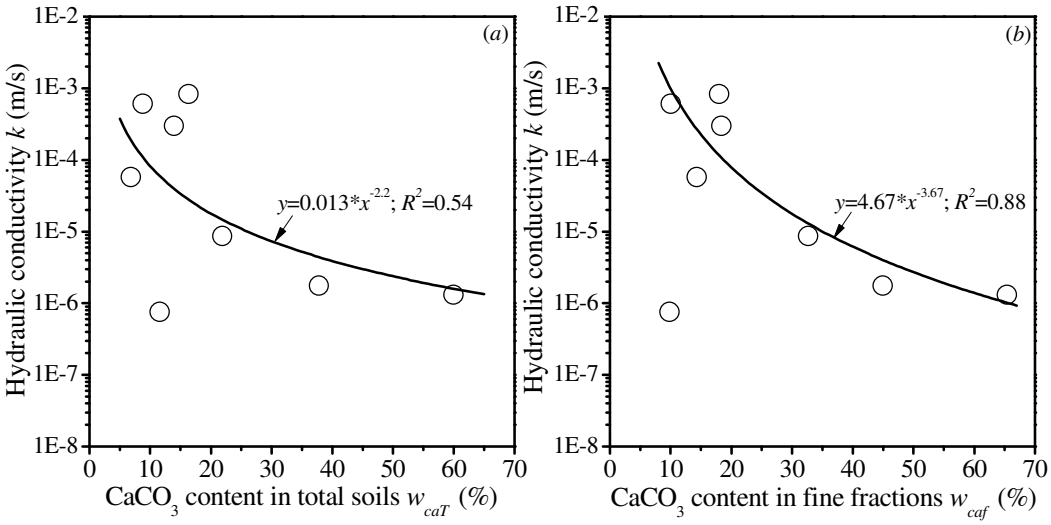

Fig. 9 Hydraulic conductivity *k vs* $CaCO_3$ content: (*a*) *k vs* w_{caT}; (*b*) *k vs* w_{caf}

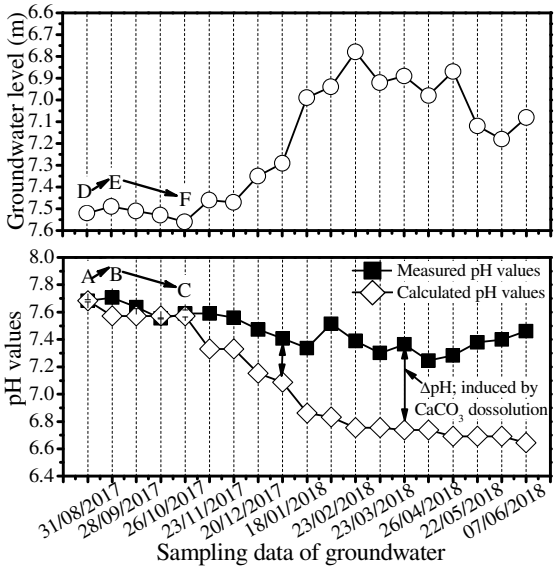

Fig. 10 Groundwater level and pH values *vs* sampling date

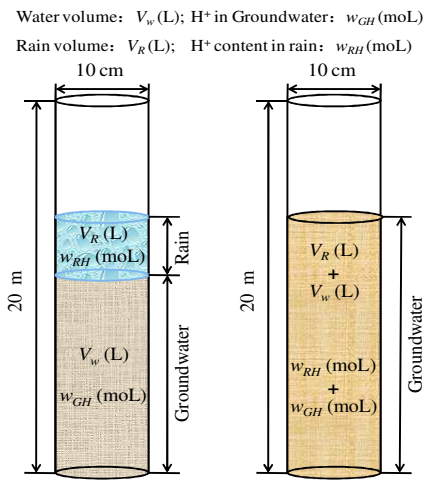

Fig. 11 Calculation model for the pH value

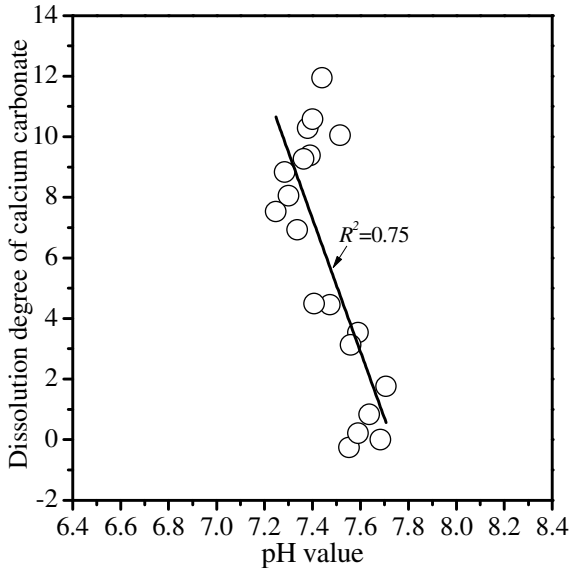

Fig. 12 Dissolution degree of calcium carbonate *vs* pH values

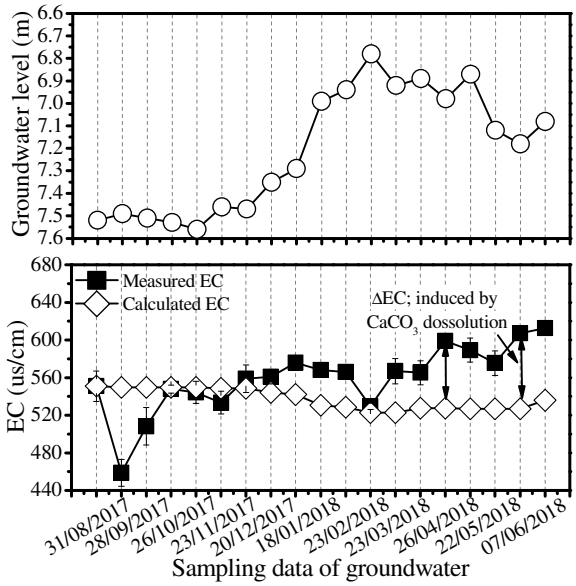

Fig. 13 Groundwater level and EC *vs* sampling date

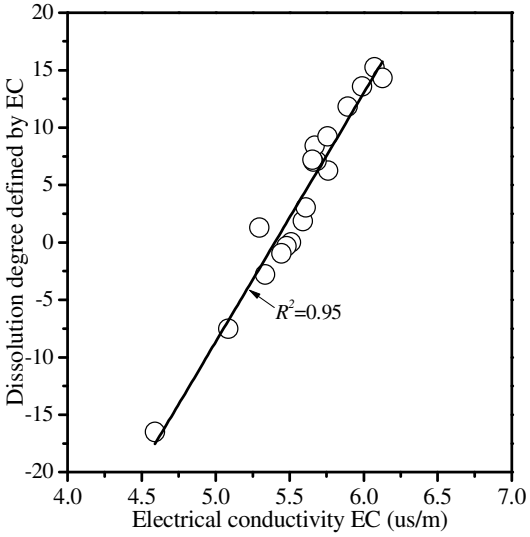

Fig. 14 Dissolution degree of calcium carbonate *vs* EC

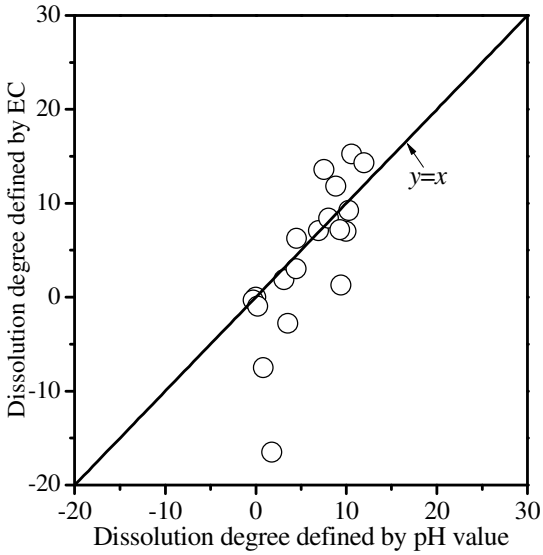

Fig. 15 Comparison of $CaCO_3$ dissolution degree